ACS APPLIED BIO MATERIALS
Article
Cite This: ACS Appl. Bio Mater. 2019, 2, 1050−1055
www.acsabm.org

Comparison of Blood−Brain Barrier Models for *in Vitro* Biological Analysis: One-Cell Type vs Three-Cell Type

Yang Song, Xiaoli Cai, Dan Du, Prashanta Dutta,* and Yuehe Lin*

School of Mechanical and Materials Engineering, Washington State University, Pullman, Washington 99164, United States

Supporting Information

ABSTRACT: Different types of *in vitro* blood−brain barrier (BBB) models have been constructed and applied for drug transport to evaluate the efficacy of nanocarrier-based drug delivery. However, the effectiveness of different types of BBB models has not been reported. In this paper, we developed two types of *in vitro* models: a one-cell type BBB model developed using only endothelial cells and a three-cell type BBB model obtained by coculturing endothelial, pericyte, and astrocyte cells. The nanoparticle transport mechanisms through the BBB and transport efficiencies of the Lactoferrin-attached silica nanoparticles were studied using both types of the *in vitro* BBB models. Compared with the one-cell type model, the PSi-Lf NPs exhibit relatively lower transport efficiency across the three-cell type BBB model. However, the effects of the nanoparticle size on the transport efficacies are consistent for both models. For both types of BBB models, the transport efficacies of the NPs are size-dependent, and the highest efficacies are achieved for PSi-Lf NPs with 25 nm in diameter. Our experimental results indicate that the one-cell type and three-cell type BBB models are equivalent for evaluating and optimizing nanoparticle transport across the BBB.

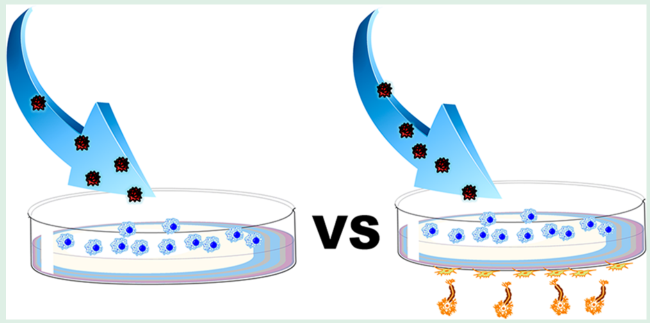

KEYWORDS: *Lactoferrin-attached silica nanoparticles, blood−brain barrier, one-cell type, three-cell type, transcytosis*

INTRODUCTION

The blood−brain barrier (BBB) is a fundamental structure for precise regulation of biomolecule transportation between the blood and the central nervous system (CNS).[1−3] Generally, it is composed of various brain endothelial cells. These cells express the low amount of leukocyte binding molecules and are capable of forming tight junctions, which limits the paracellular transportation.[4] Only several drug molecules or protein-based therapeutics could transport through the BBB freely.[5] This is because of the defense mechanism of the BBB, which protects the brain from the environmental invasion.[6,7] On the other hand, it often obstructs the delivery of brain therapeutic drugs for neurological disease treatment. Therefore, great efforts have been devoted to develop novel nanocarriers for direct brain drug delivery and improve the prognosis of patients with CNS diseases.

For nanocarrier-based targeted drug delivery, it is crucial to construct an *in vitro* model of the BBB biological system for studying the interaction between nanocarriers and the BBB. Nowadays, various kinds of *in vitro* BBB have been developed by culturing brain cells to understand the biological mechanisms of the BBB and evaluate the performance of nanocarriers.[8−10] These BBB models are usually formed using a transwell apparatus to separate the luminal side from the abluminal side.[11]

The most common model is based on growing a monolayer of BCECs on the transwell membranes (Figure 1a).[12] The one-cell type BBB model can be obtained with a relatively simple procedure and low cost.[10] However, this type of *in vitro* model is a simplified version of real BBB structure. In human and animal brains, the BBB is formed from the brain pericyte and astrocyte cells in addition to endothelial cells. Some researchers have developed *in vitro* BBB models by coculturing three types of cells (Figure 1d) to mimic the human brain.[13−16] These works demonstrated that the addition of astrocyte cells could induce more stringent interendothelial tight junctions which improves the overall expression of proprietary BBB features. The three-cell type BBB models can better mimic the BBBs in brains.[12] Despite the clear advancement in the three-cell type BBB models, these systems suffer from some disadvantages, including being expensive, and the quality of the three-cell type BBB model is more difficult to control.

In this paper, we developed two types of *in vitro* BBB models: one-cell type formed using only BCECs and three-cell type syngeneic BBB model obtained by coculturing BCECs, pericyte, and astrocyte cells. Transport of silicon nanoparticles (Si NPs) is studied through these BBB models. Since BBB endothelial cells carry a number of receptors, various ligands have been successfully used to help to transport drugs through

Received: October 26, 2018
Accepted: January 25, 2019
Published: January 25, 2019

DOI: 10.1021/acsabm.8b00654
ACS Appl. Bio Mater. 2019, 2, 1050−1055

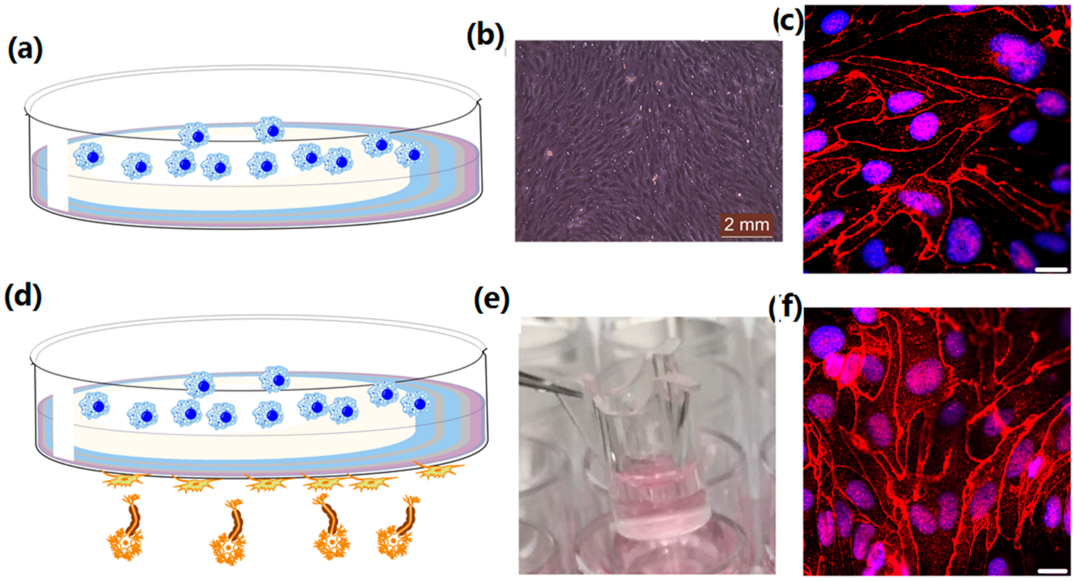

Figure 1. (a) Schematic of the one-cell type BBB model. (b) Microscopy image of the brain endothelial cells grown on the transwell membrane after day 13. (c) Immunofluorescence of membrane proteins (Claudin-5) for the one-cell type BBB model. Scale bar 20 μm. (d) Schematic of the three-cell type BBB model. (e) Photograph of a three-cell type BBB model. Reproduced with permission from ref 16. Copyright 2017, American Chemical Society. (f) Immunofluorescence of membrane proteins (Claudin-5) on a three-cell type BBB model. Scale bar 20 μm.

the BBB research.[23−25] Among them, lactoferrin (Lfs) is a mammalian cationic iron-binding glycoprotein belonging to the transferrin (Tf) family, which can bind the lactoferrin receptor on the BBB to transport across the BBB.[22] Lactoferrin-attached silica nanoparticles were used to evaluate these different BBB models. By using a combination of fluorescence imaging and permeability assay, we characterized the spatiotemporal behavior of lactoferrin-attached Si NPs transcytosis through different BBBs and identified relevant efficiencies. The results showed that NPs exhibited relatively lower transport efficiency across the three-cell type BBB system. However, the effects of the NP sizes on the transport efficacies were consistent for different models. It indicated that both types of BBB models were equally effective to optimize and select nanocarriers.

EXPERIMENTAL SECTION

Preparation of NPs. Silica nanoparticles (Si NPs) were synthesized according to the previous work.[16] Briefly, 7.5 mL of cyclohexane was mixed with Triton X-100 (1.8 mL) and *n*-hexanol (1.6 mL). For synthesis of different sizes of Si NPs, different amounts of DI water (160, 400, and 1120 μL) were added and stirred for another 20 min. Then, 80 μL of Rubpy dye (0.1 M) was injected slowly. After stirring for 5 min, 200 μL of tetraethyl orthosilicate (TEOS) and 100 μL of NH_4OH were injected. After 24 h incubation, the Si NPs were washed with DI water 3 times. Then the polyethylene glycol (PEG) labeled Si NPs (PSi NPs) and lactoferrin (Lf) attached PEG labeled Si NPs (PSi-Lf NPs) were synthesized according to a previous report.[16]

Construction of BBB Models. In this study, the one-cell type *in vitro* BBB model was formed according to a previous work.[17] This BBB model is developed by culturing the bEnd.3 endothelial cell line on the transwell membrane of microplate wells. Briefly, bEnd.3 endothelial cells were incubated on the transwell (0.4 μm pore size) with DMEM medium. Cells were grown for 13 days with changing medium every day until a compact monolayer was formed on the transwell. On the other hand, the three-cell type *in vitro* BBB model was purchased from PharmaCo-Cell Co. Ltd. (Nagasaki, Japan, http://www.pharmacocell.co.jp/, BBB kit (RBT-24H)). This BBB kit was developed by coculturing primary wistar rat BCECs, brain pericytes, and astrocytes on transwell membranes,[16] which was stored at −80 °C and can be used during one month. According to the protocol, the BBB kit has to be thawed and activated before use. The medium was defrozen in a 37 °C water bath and quickly added to the brain-side chamber and blood-side chamber. Next the BBB kit was placed in the incubator, and the medium was changed every day. After 4 days of incubation, the kit was functionally active.

Measurement of *trans*-Endothelial Electrical Resistance of BBB Models. The *trans*-endothelial electrical resistance (TEER) can be determined according to our previous study.[16] Briefly, an EVOM voltammeter with two probes was placed at both sides of the transwells. The relative resistance value was recorded as follows

$$\mathrm{TEER} = (R_A - R_Z) \times \mathrm{area} \tag{1}$$

where R_A and R_Z represent the relative resistance value and resistance of medium alone, respectively.

Transport Efficiency of Nanoparticles across BBB Models. The transport efficiency of PSi NPs or PSi-Lf NPs was calculated according to our previous study.[16] Briefly, the media containing PSi NPs and PSi-Lf NPs were incubated in the two BBB models for 12 h. Then, the medium was collected from the basolateral side, and the fluorescence intensity was recorded using fluorescence spectrometry. The transport efficiency of NPs could be determined according to this equation

$$\text{transport efficiency (\%)} = \frac{(I_b - I_c)}{(I_t - I_c)} \times 100\% \tag{2}$$

where I_b and I_t represent the collective fluorescence intensity in the basolateral side and the original medium containing PSi NPs in the apical side. I_c is calculated from autofluorescence of control.

RESULTS AND DISCUSSION

Characterization of BBB Models. As shown in Figure 1b, the brain endothelial cells, in the one-cell type BBB model, formed tight junctions with spindle-shaped optical morphology after 13 days of culture. The *trans*-endothelial electrical resistance (TEER) value is used to estimate the tightness of the BBB model. Usually, the TEER value is related with the permeability of the intercellular molecule across the BBB.[18] The strong tight junctions might eliminate all intercellular

DOI: 10.1021/acsabm.8b00654
ACS Appl. Bio Mater. 2019, 2, 1050−1055

transport mechanisms, which can result in extremely high electric resistance.[19] Previous works have demonstrated that incubation of endothelial cells on transwell could achieve a TEER value of ~200 Ω cm^2 within 12 days.[20] In this study, a TEER value of ~225 Ω cm^2 was obtained after 13 days of incubation for the one-cell type BBB model, indicating that this BBB model was suitable for *in vitro* study of the permeability assay (Figure 2). The TEER value of the BBB model formed from three types of cells is also larger than 200 Ω cm^2.[21] The immunostaining of the relative protein (Claudin-5) on one-cell type and three-cell type BBB models, as shown in Figure 1c and 1f, showed that the endothelial cells formed spindle-like junctions for both models.

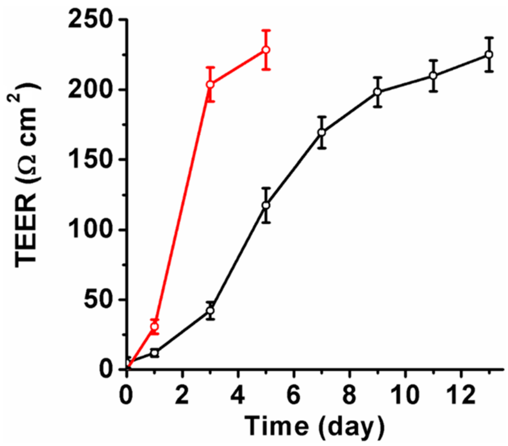

Figure 2. Measured TEER values of two types of BBB models. Black: one-cell type BBB model. Red: three-cell type BBB model. The date of TEER values of three-cell type BBB model is reproduced with permission from ref 16.

Characterization of Nanoparticles. In Figure 3a−c, the TEM images show that PSi NPs with different diameters can be successfully synthesized. The average diameter of PSi NPs is presented in the size distribution histogram (Figure 3d−f). In addition, the cytotoxicity of these NPs was evaluated. As shown in Figure 4, more than 90% cell viability on the bEnd.3 cell can be achieved after incubation with PSi NPs or PSi-Lf NPs with various concentrations for 24 h, indicating negligible cytotoxicity for these NPs.

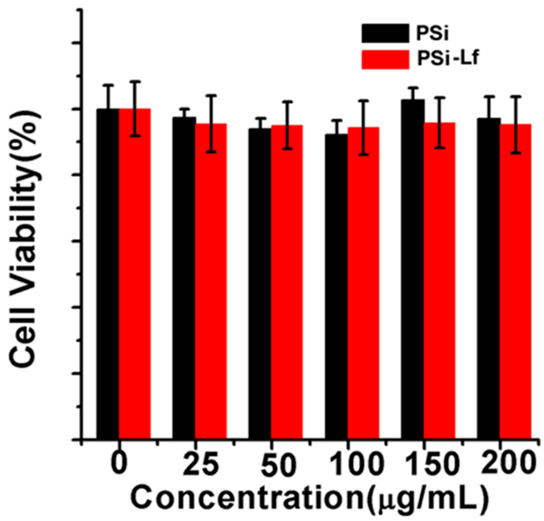

Figure 4. Cellular cytotoxicity assessment of bare PSi and lactoferrin-bound PSi nanoparticles on a one-cell type BBB model.

Transcytosis Mechanism for Different BBB Models. In earlier work,[16] we have studied the mechanism of intercellular transcytosis in the three-cell type BBB model. Briefly, we have demonstrated the transport pathway of PSi-Lf NPs during the transcytosis. The three-cell type BBB models were first

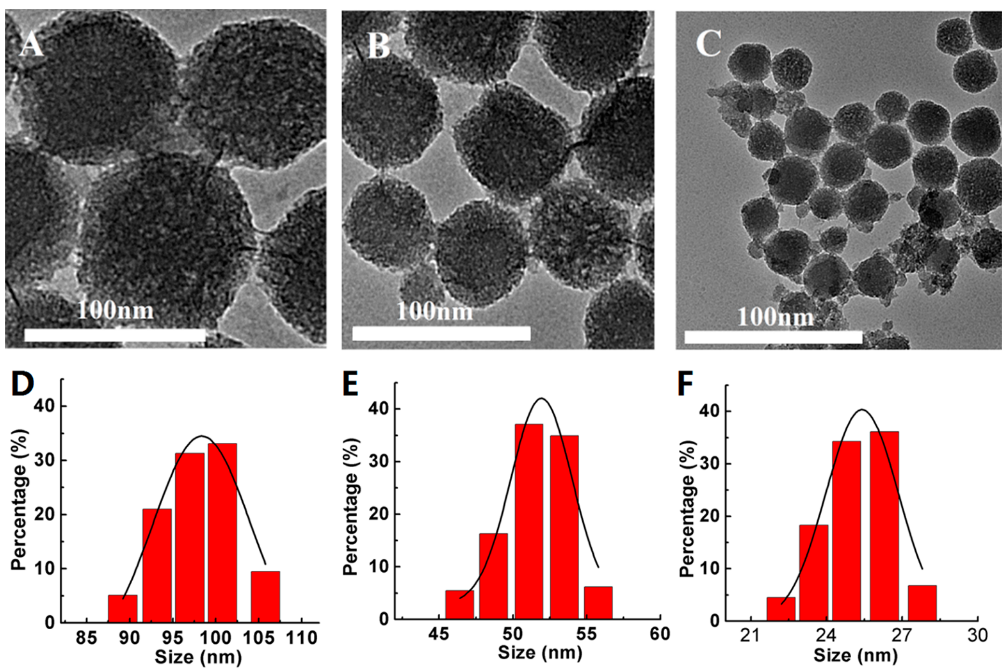

Figure 3. TEM images of (A) 100 nm, (B) 50 nm, and (C) 25 nm diameter PEG-labeled silicon nanoparticles (PSi NPs). Size distribution for (D) 100 nm, (E) 50 nm, and (F) 25 nm diameter PSi NPs.

DOI: 10.1021/acsabm.8b00654
ACS Appl. Bio Mater. 2019, 2, 1050−1055

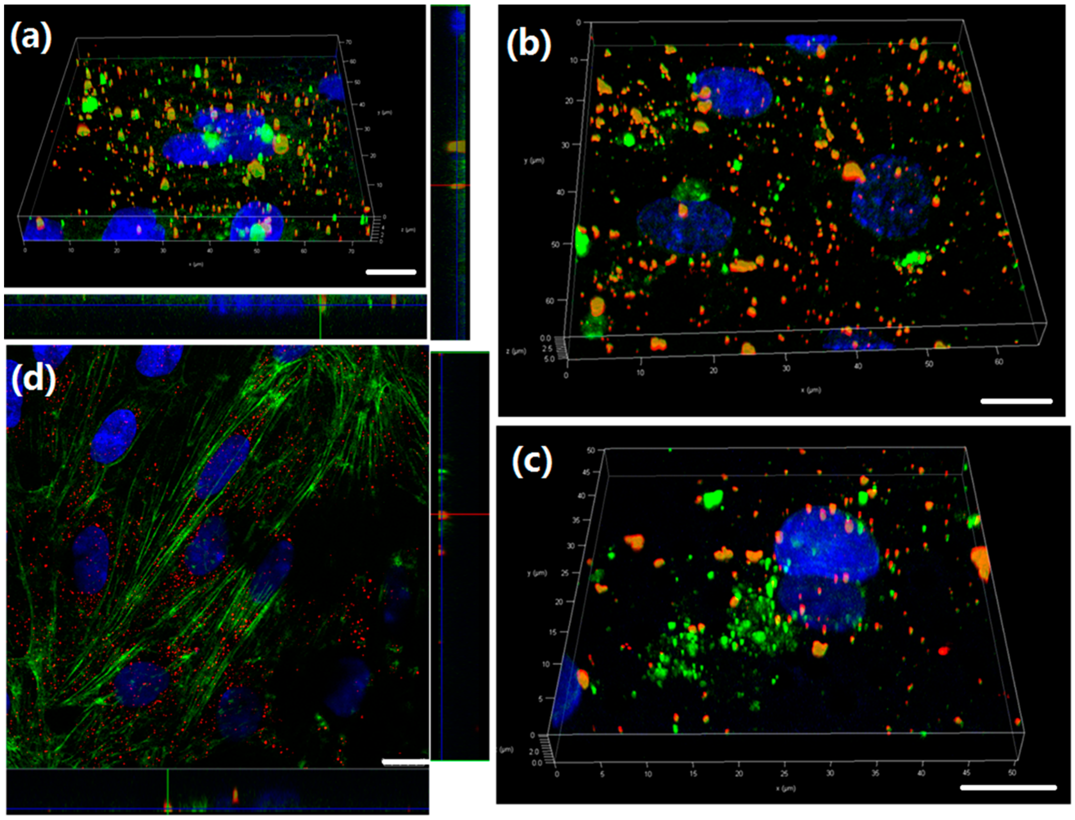

Figure 5. (a) Representative 3D confocal image showed colocalization of PSi-Lf NPs (red) and EE marker Rab-5 (green) on the one-cell type BBB model. (b) Co-localization study of PSi-Lf NPs (red) with LE marker Rab-7a (green) on the one-cell type BBB model. (c) Z-stacks reconstructed into 3D images of colocalization profiles of PSi-Lf NPs (red) with Lyso-Tracker (green) on the one-cell type BBB model. (d) Co-localization study of PSi-Lf NPs (red) with Actin (green) on the three-cell type BBB model. Reproduced with permission from ref 16. Scale bar: 10 μm.

incubated with transferrin (Tf). Figure S1a shows that endothelial cells can uptake transferrin-bound PSi-Lf NPs indicating the entry of PSi-Lf NPs through the endocytosis. After the BBB was stained with Rab 5/Rab 7, it was further incubated with PSi-Lf NPs. As shown in Figure S2a and S2b, the PSi-Lf NPs demonstrated less colocalization with early endosomes (EEs) and late endosomes (LEs), indicating the NPs trafficked backward from the EEs and LEs during the endocytosis. However, the PSi-Lf NPs showed high colocalization in the sorting endosomes (SEs) as seen in Figure S1b and S1d. Besides, the CLSM imaging indicated the colocalization of PSi-Lf NPs with the Actin network after 4 h of incubation, implying that Actin is required for efficient transcytosis and delivery in apical recycling pathways (Figure 5d). In addition, the PSi-Lf NP-containing compartment also showed less colocalization with lysosomes (Figure S1c and S1d), which indicated that the endocytosis of PSi-Lf NPs will not involve the lysosome pathway. Z-stacks reconstructed CLSM imaging, further showing transcellular movement across the BBB monolayer (Figure S2c).

In this work, we studied whether PSi-Lf NPs penetrating the one-cell BBB model exhibited the same trafficking pathway and transcytosis mechanism that was observed in the three-cell cocultured BBB model. To do so, we treated the one-cell BBB model with multiplex endocytic markers. As shown in Figure 5, the PSi-Lf NPs can colocate with the EEs after 1 h of incubation (Figure 5a) but show low colocalization with LEs after 2 h of incubation (Figure 5b), indicating PSi-Lf NPs trafficked out from EEs. Compartments containing PSi-Lf NPs were confirmed to have a low degree of association with LEs. In addition, the confocal laser scanning microscopy (CLSM) image has shown less colocalization of the PSi-Lf NPs with lysosome trackers (Figure 5c). They indicated that the transcellular mechanism of NPs on the one-cell BBB model is similar to that found in the three-cell type model.

Transport Efficiencies of Nanoparticle Across Different BBB Models. As shown in Figure 6, the transport

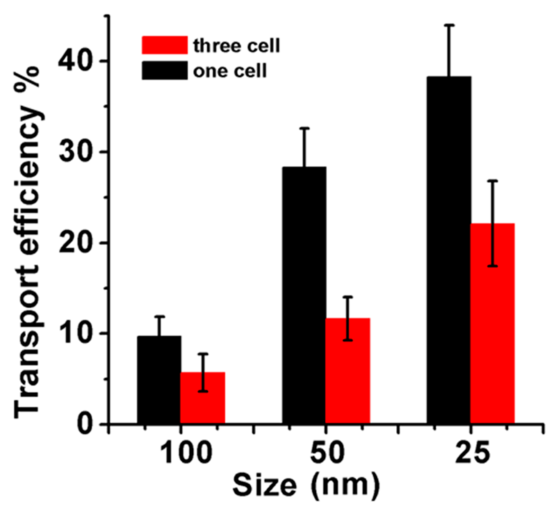

Figure 6. Transport efficiencies of PSi-Lf NPs across one-cell type and three-cells type BBB models. The date of transport efficiencies of PSi-Lf NPs across three-cell type BBB model is reproduced with permission from ref 16.

DOI: 10.1021/acsabm.8b00654
ACS Appl. Bio Mater. 2019, 2, 1050–1055

efficiency of the three-cell type BBB model demonstrated a particle size dependent transport behavior. The maximum transport efficiency was achieved for 25 nm PSi-Lf NPs among different NPs studied here (Figure 6). In the one-cell type BBB model, the 25 nm PSi-Lf NPs also achieved the highest efficiency (38%), which was 1.8-fold higher than that achieved in the three-cell type BBB model. In addition, as shown in Figure 7, the red color intensity in the BBB incubated with 25 nm PSi-Lf NPs is stronger than others (50 and 100 nm), indicating that NPs with such size achieved the most effective uptake by the endothelial cell. It is important to note that after conjugation of Lf with PSi NPs the intensity of red fluorescence in the one-cell type BBB model was strongly enhanced. The aforementioned results conclude that transport behavior of PSi-Lf NPs for the one-cell type BBB model is also size- and ligand-dependent.

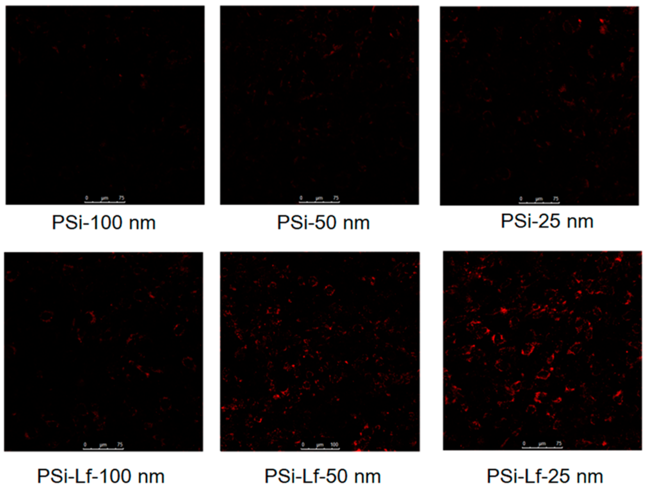

Figure 7. Confocal fluorescence images of the one-cell type BBB model *in vitro* with NPs for 2 h.

Overall, the three-cell type BBB model showed a lower permeability for NPs compared with the one-cell type BBB model. This phenomenon might be caused by the more complex astrocyte interaction and protein expression in the three-cell type BBB model. However, our results also indicate that the size-dependent nanoparticle transport trend remains the same for both BBB models. Thus, the one-cell type and three-cell type BBB models are equivalent for evaluating and optimizing NPs across the BBB. Considering the low cost and the simplicity of the construction procedure, the one-cell type BBB model is more favorable for high-throughput drug permeability test and ligand binding affinity measurement.

CONCLUSIONS

In conclusion, we compared the one-cell type and three-cell type *in vitro* BBB models. The results indicated that three-cell type cocultured BBB model offers lower permeability compared to the one-cell type BBB model. However, our results showed that the transport behavior of PSi-Lf NPs through BBB is similar for both types of BBB models. Both BBB models could be used for studying the molecular mechanisms responsible for drug permeability test and ligand binding affinity measurement.

ASSOCIATED CONTENT

Supporting Information

The Supporting Information is available free of charge on the ACS Publications website at DOI: 10.1021/acsabm.8b00654.

Additional details regarding transcytosis of lactoferrin-bound PSi-Lf NPs in the three-cell type BBB model and intracellular localization of PSi-Lf NPs in the three-cell type BBB model (PDF)

AUTHOR INFORMATION

Corresponding Authors

*E-mail: yuehe.lin@wsu.edu.
*E-mail: prashanta@wsu.edu.

ORCID

Yang Song: 0000-0003-0848-4831
Dan Du: 0000-0003-1952-4042
Yuehe Lin: 0000-0003-3791-7587

Notes

The authors declare no competing financial interest.

ACKNOWLEDGMENTS

The research reported in this publication was supported by the National Institute of General Medical Sciences of the National Institutes of Health under award number R01GM122081. The content is solely the responsibility of the authors and does not necessarily represent the official views of the National Institutes of Health.

REFERENCES

(1) Ballabh, P.; Braun, A.; Nedergaard, M. The Blood-Brain Barrier: An Overview: Structure, Regulation, and Clinical Implications. *Neurobiol. Dis.* **2004**, *16* (1), 1−13.

(2) Farrall, A. J.; Wardlaw, J. M. Blood-Brain Barrier: Ageing and Microvascular Disease-Systematic Review and Meta-Analysis. *Neurobiol. Aging* **2009**, *30* (3), 337−352.

(3) Hawkins, B. T.; Davis, T. P. The Blood-Brain Barrier/Neurovascular Unit in Health and Disease. *Pharmacol Rev.* **2005**, *57* (2), 173.

(4) Abbott, N. J.; Ronnback, L.; Hansson, E. Astrocyte-Endothelial Interactions at the Blood-Brain Barrier. *Nat. Rev. Neurosci.* **2006**, *7* (1), 41−53.

(5) Calvo, P.; Gouritin, B.; Chacun, H.; Desmaële, D.; D'Angelo, J.; Noel, J.-P.; Georgin, D.; Fattal, E.; Andreux, J. P.; Couvreur, P. Long-Circulating PEGylated Polycyanoacrylate Nanoparticles as New Drug Carrier for Brain Delivery. *Pharm. Res.* **2001**, *18* (8), 1157−1166.

(6) Begley, D. J. Delivery of Therapeutic Agents to the Central Nervous System: the Problems and the Possibilities. *Pharmacol. Ther.* **2004**, *104* (1), 29−45.

(7) Orive, G.; Ali, O. A.; Anitua, E.; Pedraz, J. L.; Emerich, D. F. Biomaterial-Based Technologies for Brain Anti-Cancer Therapeutics and Imaging. *Biochim. Biophys. Acta, Rev. Cancer* **2010**, *1806* (1), 96−107.

(8) Bramini, M.; Ye, D.; Hallerbach, A.; Nic Raghnaill, M.; Salvati, A.; Åberg, C.; Dawson, K. A. Imaging Approach to Mechanistic Study of Nanoparticle Interactions with the Blood-Brain Barrier. *ACS Nano* **2014**, *8* (5), 4304−4312.

(9) Schiera, G.; Sala, S.; Gallo, A.; Raffa, M. P.; Pitarresi, G. L.; Savettieri, G.; Liegro, I. D. Permeability Properties of a Three-Cell Type In Vitro Model of Blood-Brain Barrier. *J. Cell. Mol. Med.* **2005**, *9* (2), 373−379.

(10) Naik, P.; Cucullo, L. In Vitro Blood−Brain Barrier Bodels: Current and Perspective Technologies. *J. Pharm. Sci.* **2012**, *101* (4), 1337−1354.

(11) Rubin, L. L.; Hall, D. E.; Porter, S.; Barbu, K.; Cannon, C.; Horner, H. C.; Janatpour, M.; Liaw, C. W.; Manning, K.; Morales, J. A Cell Culture Model of the Blood-Brain Barrier. *J. Cell Biol.* **1991**, *115* (6), 1725−1735.

(12) Abbott, N. J.; Rönnbäck, L.; Hansson, E. Astrocyte-Endothelial Interactions at the Blood-Brain Barrier. *Nat. Rev. Neurosci.* **2006**, *7*, 41.

(13) Hayashi, K.; Nakao, S.; Nakaoke, R.; Nakagawa, S.; Kitagawa, N.; Niwa, M. Effects of Hypoxia on Endothelial/Pericytic Co-culture Model of the Blood-Brain Barrier. *Regul. Pept.* **2004**, *123* (1), 77−83.

(14) Stanness, K. A.; Neumaier, J. F.; Sexton, T. J.; Grant, G. A.; Emmi, A.; Maris, D. O.; Janigro, D. A New Model of the Blood-Brain Barrier: Co-culture of Neuronal, Endothelial and Glial Cells under Dynamic Conditions. *NeuroReport* **1999**, *10* (18), 3725−3731.

(15) Megard, I.; Garrigues, A.; Orlowski, S.; Jorajuria, S.; Clayette, P.; Ezan, E.; Mabondzo, A. S. A Co-culture-based Model of Human Blood-Brain Barrier: Application to Active Transport of Indinavir and In Vivo-In Vitro Correlation. *Brain Res.* **2002**, *927* (2), 153−167.

(16) Song, Y.; Du, D.; Li, L.; Xu, J.; Dutta, P.; Lin, Y. In Vitro Study of Receptor-Mediated Silica Nanoparticles Delivery across Blood-Brain Barrier. *ACS Appl. Mater. Interfaces* **2017**, *9* (24), 20410−20416.

(17) Wong, A. D.; Ye, M.; Levy, A. F.; Rothstein, J. D.; Bergles, D. E.; Searson, P. C. The Blood-Brain Barrier: An Engineering Perspective. *Front. Neuroeng.* **2013**, *6*, 1−22.

(18) Singh, A. V.; Batuwangala, M.; Mundra, R.; Mehta, K.; Patke, S.; Falletta, E.; Patil, R.; Gade, W. N. Biomineralized Anisotropic Gold Microplate-Macrophage Interactions Reveal Frustrated Phagocytosis-like Phenomenon: A Novel Paclitaxel Drug Delivery Vehicle. *ACS Appl. Mater. Interfaces* **2014**, *6* (16), 14679−14689.

(19) Lohmann, C.; Hüwel, S.; Galla, H. J. Predicting Blood-Brain Barrier Permeability of Drugs: Evaluation of Different In Vitro Assays. *J. Drug Target* **2002**, *10* (4), 263−276.

(20) Hanada, S.; Fujioka, K.; Inoue, Y.; Kanaya, F.; Manome, Y.; Yamamoto, K. Cell-Based in Vitro Blood-Brain Barrier Model Can Rapidly Evaluate Nanoparticles' Brain Permeability in Association with Particle Size and Surface Modification. *Int. J. Mol. Sci.* **2014**, *15*, 1812−1825.

(21) Nurunnabi, M.; Khatun, Z.; Huh, K. M.; Park, S. Y.; Lee, D. Y.; Cho, K. J.; Lee, Y. K. In Vivo Biodistribution and Toxicology of Carboxylated Graphene Quantum Dots. *ACS Nano* **2013**, *7* (8), 6858−6867.

(22) Hu, K.; Li, J.; Shen, Y.; Lu, W.; Gao, X.; Zhang, Q.; Jiang, X. Lactoferrin-Conjugated PEG-PLA Nnanoparticles with Improved Brain Delivery: In Vitro and In Vivo Evaluations. *J. Controlled Release* **2009**, *134* (1), 55−61.

(23) Tian, X.; Nyberg, S.; Sharo, P. S.; Madsen, J.; Daneshpour, N.; Steven, P. A.; Berwick, J.; Azzouz, M.; Shaw, P.; Abbott, N. J.; Battaglia, G. LRP-1-Mediated Intracellular Antibody Delivery to the Central Nervous System. *Sci. Rep.* **2015**, *5*, 11990.

(24) Huang, R.; Ke, W.; Liu, Y.; Jiang, C.; Pei, Y. The Use of Lactoferrin as A Ligand for Targeting the Polyamidoamine-Based Gene Delivery System to the Brain. *Biomaterials* **2008**, *29*, 238−246.

(25) Huang, R.; Ke, W.; Han, L.; Liu, Y.; Shao, K.; Jiang, C.; Pei, Y. Lactoferrin-Modified Nanoparticles Could Mediate Efficient Gene Delivery to the Brain In Vivo. *Brain Res. Bull.* **2010**, *81*, 600−604.

DOI: 10.1021/acsabm.8b00654
ACS Appl. Bio Mater. 2019, 2, 1050−1055